Supplementary Information (SI) for Analyst.
This journal is © The Royal Society of Chemistry 2024

Characterization of Vaginal Lactobacillus in Biologically Relevant Fluid using Surface-Enhanced Raman Spectroscopy

Anna S. Rourke-Funderburg[a,b], Anita Mahadevan-Jansen[a,b], Andrea K. Locke[a,b,c]*

[a]Department of Biomedical Engineering, Vanderbilt University

[b]Vanderbilt Biophotonics Center, Vanderbilt University

[c]Department of Chemistry, Vanderbilt University

*corresponding author: andrea.locke@vanderbilt.edu

Transmission Electron Microscopy

L. crispatus cultures were grown following procedures outlined previously. Liquid cultures were washed via centrifugation at 3,300g for 8 minutes and resuspended with sterile DI water. Washed cultures and AuNPs were mixed at a 1:4 volumetric ratio (bacteria:AuNPs) by pipetting and were vortexed for 2-3 seconds to ensure homogenous mixing. The solution was allowed to sit for 15 minutes to allow for AuNPs and bacteria interaction. Following the 15-minute interaction period, the solution was centrifuged at 725 RCF for 15 minutes and the supernatant was replaced with 2.5% glutaraldehyde for bacterial cell fixation. The solution was fixed in glutaraldehyde for 30 minutes before a 5 µL droplet was applied to a TEM grid (Ted Pella; Redding, CA). The grid was allowed to dry for 30 minutes then washed with DI water twice. The grid was allowed to fully dry before being imaged using a Tecnai Osiris TEM (Thermo Fisher Scientific, Waltham, MA) at 3,600X and 6,300X magnification with 200 kV accelerating voltage and a 1 second integration time.

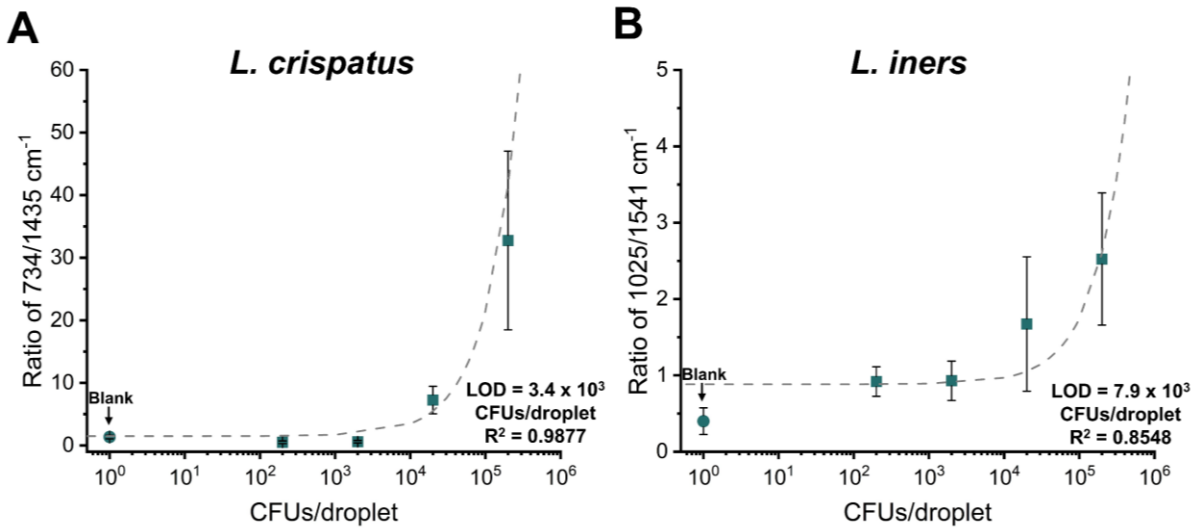

Supplemental Figure 1. Scatter plots of ratiometric values used to calculate the limit of detection (LOD) of (A) *L. crispatus* and (B) *L. iners* with goodness of fit (R^2) reported.

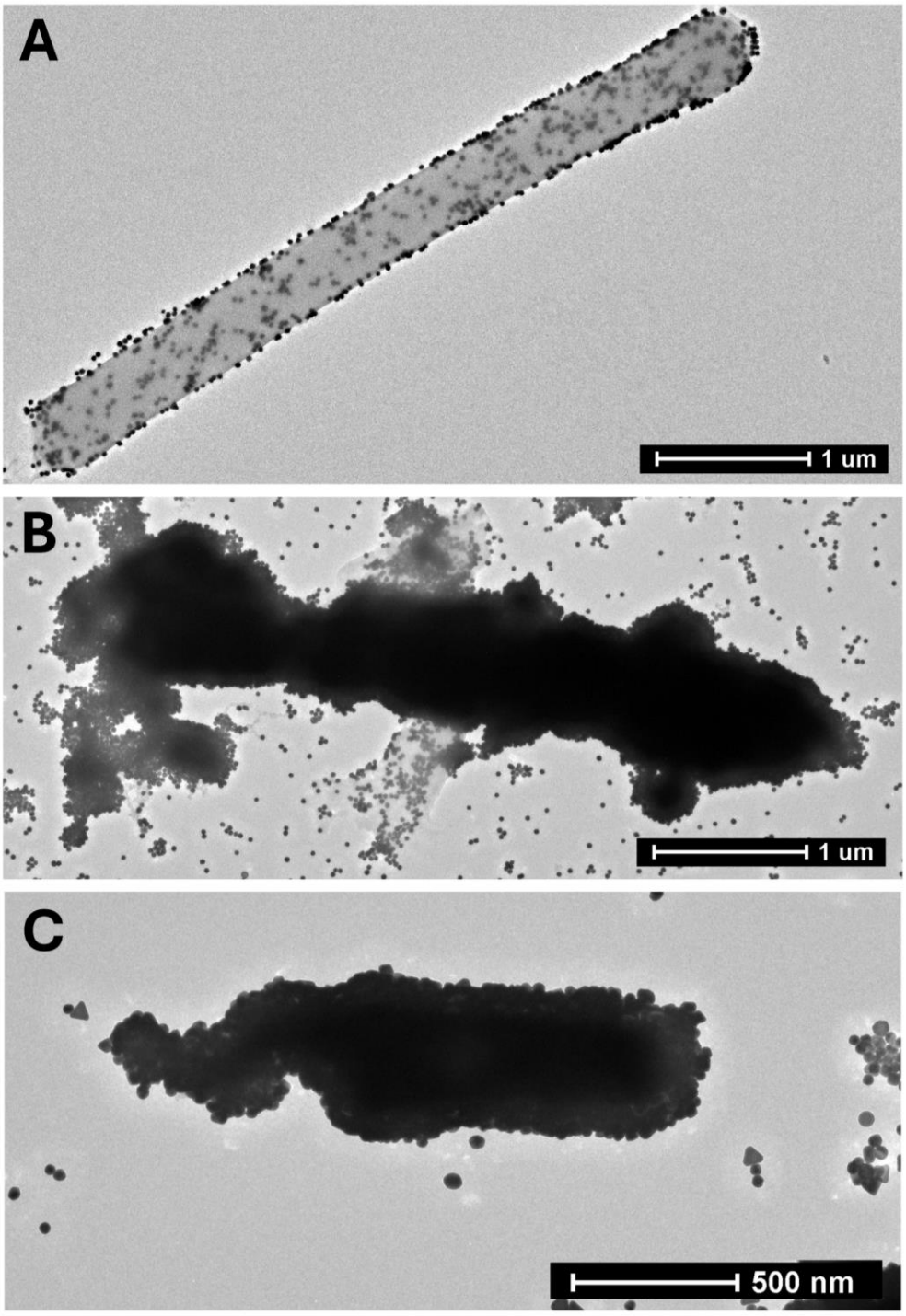

Supplemental Figure 2. TEM images of *L. crispatus* and *L. iners* cells at varying bacterial concentrations showing variations in the density of AuNPs attached to the bacterial cell wall and differing cell morphology: (A) *L. crispatus*, 2 x 10^5 CFUs/droplet, 3600X magnification; (B) *L. crispatus*, 2 x 10^3 CFUs/droplet, 3600X magnification; (C) *L. iners*, 2 x 10^3 CFUs/droplet, 6300X magnification.

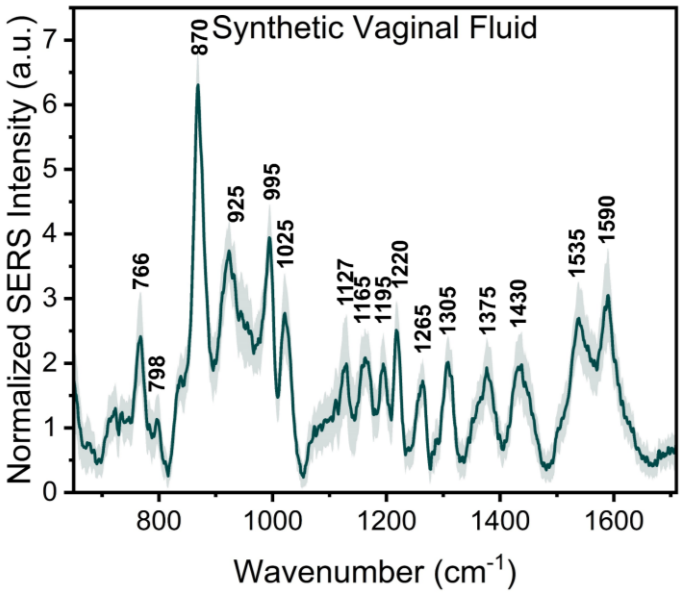

WVN (cm^{-1})	Tentative Peak Origin
766	Amino acids[1]
798	Proteins[1], glucose[2]
870	Amino acids[1], glucose[2]
923-930	Lactic acid[3], acetic acid[1]
995	Phenylalanine[1]
1025	Proteins[4]
1127	Proteins[1], lactic acid[3], glucose[2,5]
1165	Amino acids[1]
1195	Amino acids[6]
1220	Amino acids[1]
1265	Glucose[5]
1305	Amide III (proteins)[7]
1375	Glycerol[8]
1430	Amino acids[1]
1535-1590	Amino acids[1,9], Lactic acid[3]

Supplemental Figure 3. SERS spectrum of SVF. Each spectra is the mean and standard deviation (represented by shaded error bars) of 3 experimental replicates [n=45 spectra]) and table of peak origins for the highlighted peaks.

Supplemental Table 1. Table of wavenumber assignments of peaks with VIP value greater than 1 in both PLSR models.

WVN (cm^{-1})	Pure or Complex	Tentative assignment
734	Both	C-N stretching, the glycosidic ring vibrations, or in plane breathing mode of adenine[10-13]
768	Pure	Indole ring breathing/stretching[6, 16, 17]
865	Complex	Indole ring scissoring, indole N-H displacement, indole ring vibration with N-H bending, C-H stretching[1,2,14]
962	Pure	C=C deformation, C-N stretching, C-O stretching, CH_3 symmetric stretching [11]
989-998	Both	Phenyl ring angular bending vibrations[15]
1025	Complex	C-N or C-C stretching, or C-H in plane bending[11]
1315-1320	Both	CH_3CH_2 vibrations, Amide III[6]
1340	Pure	CH_3CH_2 wagging, Amide III, CH_2 wagging, C-H deformation[6]
1380-1390	Complex	CH_3, C-H, C-N vibrations[6]
1430-1440	Both	CH_2 scissoring and deformation[6]
1457-1468	Complex	CH_2 and C-H vibrations[11]
1535	Pure	Amide carbonyl group vibrations[6]
1560	Pure	Amide I, C=O stretching, C=C bending [11]

References:

1 G. P. Szekeres and J. Kneipp, *Front Chem*, 2019, **7**, 434849.

2 T. T. B. Quyen, W. N. Su, K. J. Chen, C. J. Pan, J. Rick, C. C. Chang and B. J. Hwang, *Journal of Raman Spectroscopy*, 2013, **44**, 1671–1677.

3 M. Verma, T. K. Naqvi, S. K. Tripathi, M. M. Kulkarni, N. E. Prasad and P. K. Dwivedi, *IEEE Trans Nanobioscience*, 2022, **21**, 294–300.

4 S. Bashir, H. Nawaz, M. Irfan Majeed, M. Mohsin, A. Nawaz, N. Rashid, F. Batool, S. Akbar, M. Abubakar, S. Ahmad, S. Ali and M. Kashif, *Spectrochim Acta A Mol Biomol Spectrosc*, 2021, **258**, 119831.

5 O. Lyandres, N. C. Shah, C. R. Yonzon, J. T. Walsh, M. R. Glucksberg and R. P. Van Duyne, *Anal Chem*, 2005, **77**, 6134–6139.

6 Z. Movasaghi, S. Rehman and I. U. Rehman, *Appl Spectrosc Rev*, 2007, **42**, 493–541.

7 X. Yu, W. Li, O. Liang, Y. Bai and Y. hong Xie, *Anal Biochem*, 2020, **599**, 113709.

8 A. C. De Luca, P. Reader-Harris, M. Mazilu, S. Managò, S. Mariggiò, D. Corda and A. Di Falco, in *SPIE BiOS: Plasmonics in Biology and Medicine XI*, SPIE, 2014, vol. 8957, p. 895709.

9 W. Xiaodan, Z. Dawei, Z. Ping, L. Taifeng, W. Huiqin and Z. Yongwei, *J Appl Biomater Funct Mater*, 2018, **16**, 157–162.

10 W. R. Premasiri, J. C. Lee, A. Sauer-Budge, R. Theberge, C. E. Costello, L. D. Ziegler and D. Fraunhofer, *Anal Bioanal Chem*, 2016, **408**, 4631–4647.

11 S. M. Berus, M. Adamczyk-Popławska, K. Goździk, G. Przedpełska, T. R. Szymborski, Y. Stepanenko and A. Kamińska, *Int J Mol Sci*, 2022, **23**, 12576.

12 S. Efrima and L. Zeiri, *Journal of Raman Spectroscopy*, 2009, **40**, 277–288.

13 P. Kubryk, R. Niessner and N. P. Ivleva, *Analyst*, 2016, **141**, 2874.

14 G. Pezzotti, *Journal of Raman Spectroscopy*, 2021, **52**, 2348–2443.

15 B. Hernández, F. Pflüger, S. G. Kruglik and M. Ghomi, *Journal of Raman Spectroscopy*, 2013, **44**, 827–833.

16 I. A. Boginskaya, E. A. Slipchenko, M. V. Sedova, J. Y. Zvyagina, A. D. Maximov, A. S. Baburin, I. A. Rodionov, A. M. Merzlikin, I. A. Ryzhikov and A. N. Lagarkov, *Chemosensors*, 2023, **11**, 321.

17 S. Stewart and P. M. Fredericks, *Spectrochim Acta A Mol Biomol Spectrosc*, 1999, **55**, 1641–1660.